**PAPER**

Check for updates

# Radical-cation salts of BEDT-TTF with tris-coordinated racemic dysprosium(III) and terbium(III) anions†

Emily Howarth,[a] Jordan Lopez,[a] Joseph O. Ogar, [ID] [a] Toby J. Blundell, [ID] [a] Hiroki Akutsu, [ID] [b] Yasuhiro Nakazawa,[b] Shusaku Imajo,[c] Yoshihiko Ihara,[d] Simon J. Coles, [ID] [e] Peter N. Horton,[e] Jeppe Christensen[e] and Lee Martin [ID] *[a]

This paper reports the synthesis, crystal structures and conducting properties of the first BEDT-TTF radical-cation salts with $D_3$ symmetry tris-coordinated racemic lanthanide(III) anions. It is also the first crystallographic determination of the nine-coordinate tris(chelidonato)terbate and tris(chelidonato)dysprosate anions (chelidonic acid = clo = 4-oxo-4H-pyran-2,6-dicarboxylic acid). Salt α-(BEDT-TTF)$_5$M(chelidonato)$_3$·EtOH·2H$_2$O is semimetallic for M = **Tb**, and semiconducting for M = **Dy**. These conducting properties are consistent with the band structure for both salts.

## Introduction

Radical-cation salts of the donor molecule BEDT-TTF [bis(ethylenedithio)tetrathiafulvalene] form two-dimensional conducting donor layers which alternate with the insulating anion layers.[1] They show great variety in their crystal packing arrangements and their conducting properties. The insulating anion layer offers the opportunity to introduce molecules with a 2nd property to the conducting material. The possibility of combining magnetism with conductivity or superconductivity in these materials has been widely explored by introducing transition metals into the anion layer.[2]

The metallic radical-cation salt (BEDT-TTF)$_3$CuCl$_4$·H$_2$O was the first example of the coexistence of localised and conduction electrons in the same material.[3] The discovery of the first paramagnetic superconductor β″-(BEDT-TTF)$_4$(H$_3$O)Fe(C$_2$O$_4$)$_3$·C$_6$H$_5$CN[4] led to a family of salts containing the tris(oxalato)metallate(III) anion which has the ability to bridge with mono-cations or metal(II) ions to give long-range magnetic order. As well as producing the first ferromagnetic metal
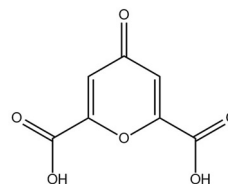


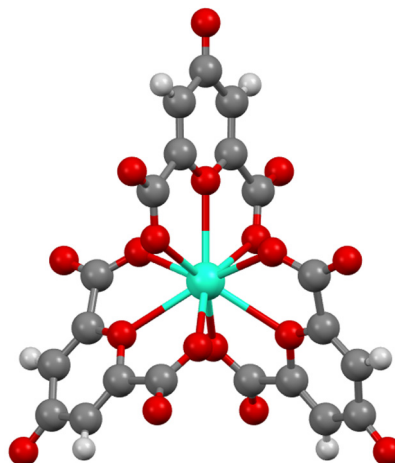**Scheme 1** Chelidonic acid (clo = 4-oxo-4H-pyran-2,6-dicarboxylic acid).

[a]School of Science and Technology, Nottingham Trent University, Clifton Lane, Clifton, Nottingham, NG11 8NS, UK. E-mail: lee.martin@ntu.ac.uk

[b]Department of Chemistry, Graduate School of Science, Osaka University, 1-1 Machikaneyama-cho, Toyonaka, Osaka 560-0043, Japan

[c]The Institute for Solid State Physics, The University of Tokyo, Kashiwa, Chiba 277-8581, Japan

[d]Department of Quantum and Condensed Matter Physics, School of Science, Hokkaido University, Kita-ku, Sapporo, 060-0810 Hokkaido, Japan

[e]School of Chemistry, Faculty of Natural and Environmental Sciences, University of Southampton, Highfield, Southampton, SO17 1BJ, UK

†Electronic supplementary information (ESI) available. CCDC 2357688 for **Tb** and 2357687 for **Dy**. For ESI and crystallographic data in CIF or other electronic format see DOI: https://doi.org/10.1039/d4dt03484h
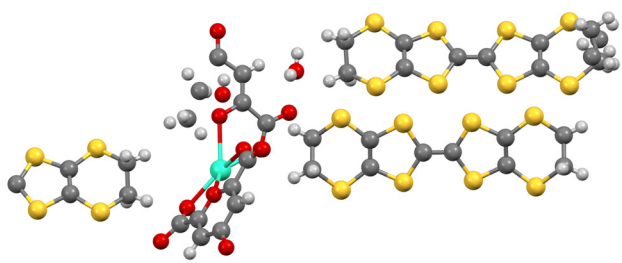


**Fig. 1** Structure of the Ln(clo)$_3$$^{3-}$ anion.

**Fig. 2** Asymmetric unit (M = **Dy** shown).

**Table 1** X-ray data for salts **Tb** and **Dy**

|  | Tb | Dy |
|---|---|---|
| Formula | $C_{73}H_{56}O_{21}S_{40}Tb_1$ | $C_{73}H_{56}O_{21}S_{40}Dy_1$ |
| $F_w$ [g mol$^{-1}$] | 2710.56 | 2714.07 |
| Crystal system | Monoclinic | Monoclinic |
| Space group | $C2/c$ | $C2/c$ |
| $Z$ | 4 | 4 |
| $T$ (K) | 293.1(7) | 30(2) |
| $a$ [Å] | 47.654(2) | 44.9281(9) |
| $b$ [Å] | 11.0579(3) | 11.0132(2) |
| $c$ [Å] | 21.3658(9) | 20.9971(4) |
| $\alpha$ [°] | 90 | 90 |
| $\beta$ [°] | 120.249(6) | 113.191(2) |
| $\gamma$ [°] | 90 | 90 |
| Volume [Å$^3$] | 9725.9(9) | 9549.9(3) |
| Density [g cm$^{-3}$] | 1.851 | 1.888 |
| $\mu$ [mm$^{-1}$] | 1.653 | 1.723 |
| $R_1$ | 0.0468 | 0.0502 |
| $wR$ [all data] | 0.1037 | 0.1268 |

β-(BEDT-TTF)$_3$[MnCr(C$_2$O$_4$)$_3$],[5] and an antiferromagnetic semiconductor (BEDT-TTF)$_3$Cu$_2$(C$_2$O$_4$)$_3$·(CH$_3$OH)$_2$,[6] a number of conducting salts in this family have been obtained by using other 3d, 4d, 5d, or main group metal centres (M = Cr, Co, Mn, Al, Ga, Ge, Ru, Rh, Ir).[7]
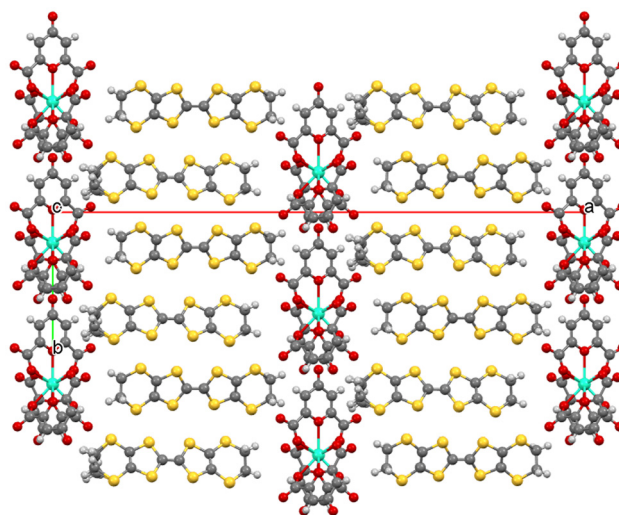


**Fig. 4** Structure viewed down the *c* axis (M = **Dy** shown).

There are very few 4f–π systems and the number of rare-earth anions that have previously been included in radical-cation salts of BEDT-TTF is limited to only a few examples. [Ln(NCS)$_6$]$^{3-}$ anions (Ln = Ho, Er, Yb or Y) have produced semiconducting salts of (BEDT-TTF)$_4$[Ln(NCS)$_6$]·CH$_2$Cl$_2$;[8] [Ln(NCS)$_6$NO$_3$]$^{4-}$ anions (Ln = Dy, Ho, Er, Yb or Y) have produced semiconducting salts of (BEDT-TTF)$_5$[Ln(NCS)$_6$NO$_3$]·EtOH;[9] and (BEDT-TTF)$_5$[Dy(NO$_3$)$_4$] shows a metal–insulator phase transition at ~200 K.[10] Metallic radical-cation salts have been reported using [Ln(NCS)$_6$]$^{3-}$ or [Ln(NCS)$_6$NO$_3$]$^{4-}$ anions with the cations BO, DIEDO, or TTP.[11] Recently, semiconducting 4f–π systems have combined BEDT-TTF with SMMs in [β′-(BEDT-TTF)$_2$Dy(hfac)$_4$·MeCN]$_n$ and κ-(BEDT-TTF)$_5$[Dy(NCS)$_7$]·(KCl)$_{0.5}$ which show slow relaxation of the magnetisation and electrical conductivity.[12]
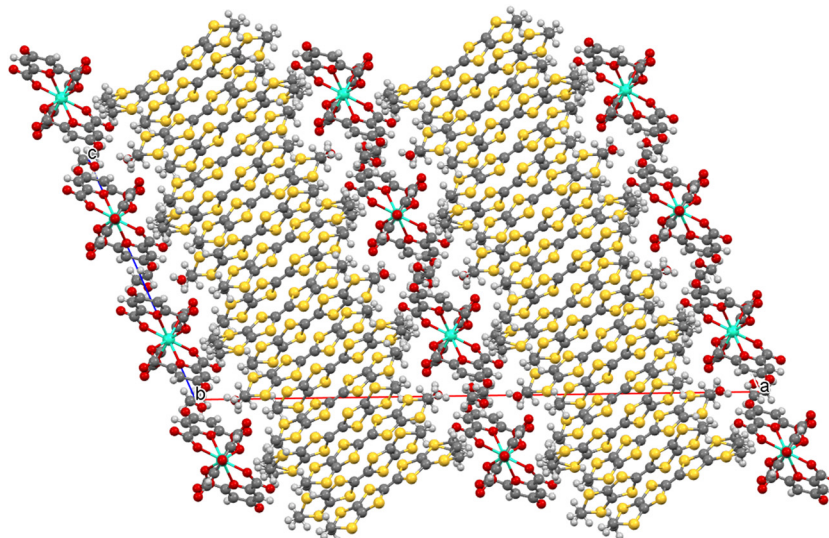


**Fig. 3** Structure viewed down the *b* axis (M = **Dy** shown).

**Dalton Transactions**     **Paper**

This paper reports the first use of a racemic propeller-shaped lanthanide anion in a radical-cation salt with BEDT-TTF. Three tridentate chelidonic acid ligands (clo = 4-oxo-4$H$-pyran-2,6-dicarboxylic acid, Scheme 1) produce a nine-coordinate lanthanide anion having $D_3$ symmetry with the two carboxylate groups and the ring oxygen atom providing the donor atoms (Fig. 1). Nine-coordinate tris(chelidonato) lanthanide anions have previously been studied spectroscopically,[13] and the chelidonate ligand has been employed extensively in coordination polymers with lanthanides.[14] The anion $[Dy(cla)_3]^{3-}$ from chelidamic acid (cla = 4-hydroxypyridine-2,6-dicarboxylate) crystallises with $[Dy(H_2O)_4]^{3+}$ in MOF $\{[Dy_2(cla)_3(H_2O)_4]\cdot 2H_2O\}_n$,[15] however, to the best of our knowledge this paper reports the first crystallographic observation of the $[Dy(clo)_3]^{3-}$ and $[Tb(clo)_3]^{3-}$ anions.

The use of tris(oxalato)metallates with $D_3$ symmetry in BEDT-TTF radical-cation salts produces a wide range of packing arrangements.[5] The distribution of the enantiomers of $[M(C_2O_4)_3]^{3-}$ anions leads to different polymorphs with different conducting behaviours.[4,5] Chiral induction has also produced salts where only a single enantiomer of the labile $[M(C_2O_4)_3]^{3-}$ anion is present,[16] and the use of $[Ln(clo)_3]^{3-}$ anions here also offers the potential to introduce chirality into these multifunctional materials.[17] The bulky size of the $[Ln(clo)_3]^{3-}$ anions compared to $[M(C_2O_4)_3]^{3-}$ also gives the potential for wide insulating layers and the synthesis of 2D superconductors.[18]

## Results and discussion

### α-(BEDT-TTF)$_5$M(clo)$_3$·EtOH·2H$_2$O (M = Tb or Dy)

Salts **Tb** and **Dy** are isomorphous and crystallise in the monoclinic space group $C2/c$ (Fig. 2)(Table 1). The asymmetric unit contains two and a half BEDT-TTF molecules, half a Ln(clo)$_3$ anion, a molecule of water, and half a molecule of ethanol. The ethanol molecule is disordered over two positions forming hydrogen bonds with the 4-oxo carbonyl of chelidonate ligands.
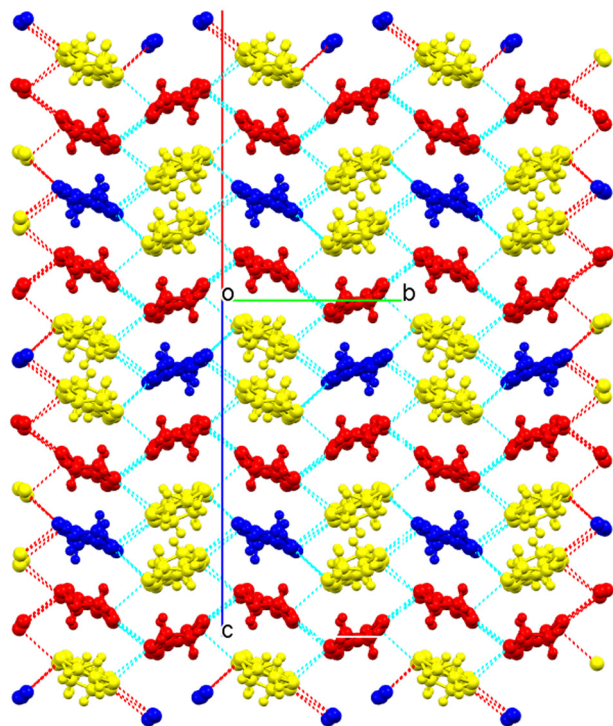


**Fig. 5** Packing arrangement of donor layer showing S···S close contacts and symmetry equivalent BEDT-TTF molecules (donor A = yellow, B = red, C = blue) (M = **Dy** shown).
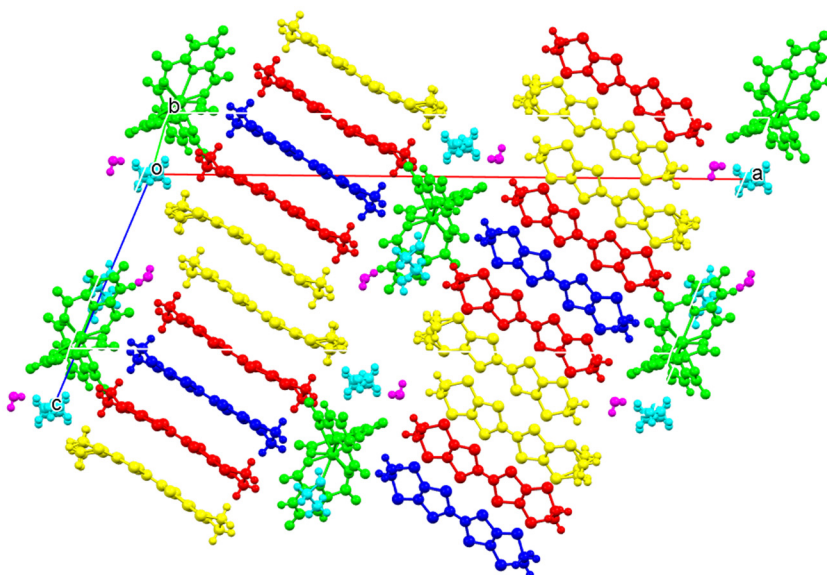


**Fig. 6** Structure viewed down the $b$ axis showing symmetry equivalent BEDT-TTF molecules (donor A = yellow, B = red, C = blue) (M = **Dy** shown).

Fig. 3 and 4 shows the layered packing of these salts which consists of donor layers of BEDT-TTF separated by anion layers of $[Ln(clo)_3]^{3-}$/ethanol/water. There are two donor layers in the unit cell but both are crystallographically the same and related by a two-fold axis. The donors stack in the *bc* plane in an α packing motif (Fig. 5). Within a stack of donors in the *c* direction the donors are arranged in an .. ABCBAABCBA.. repeating pattern (Fig. 6) to form a pentamer
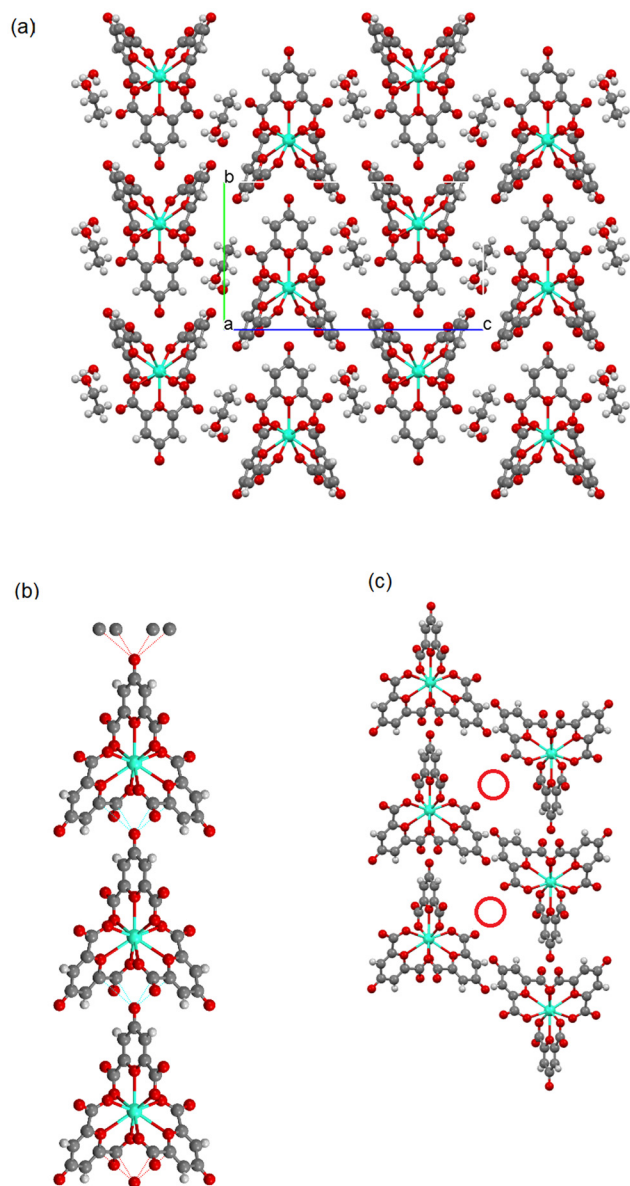


**Fig. 7** (a) Packing arrangement of anion layer viewed down the *a* axis (M = **Dy** shown) showing rows of a single enantiomer of $[Ln(clo)_3]^{3-}$ anion in the *b* direction. The adjacent rows in the *c* direction in this figure follow the pattern Λ−Δ−Λ−Δ from left to right. (b) The dashed lines within a single row of anions indicates the short contacts between O9 and C26/C27 forming 1D chains of the anion. (c) The red circle indicates the location where the ethylene group of the BEDT-TTF molecule of the pentamer is located.

(Fig. 6 and 7), in which 3 holes are located according to the charge balance. There are multiple side-to-side S···S interactions between neighbouring donor stacks below the sum of the van der Waals radii (Table 2 and Fig. 5), with no face-to-face S···S interactions. Applying the method from Guionneau *et al.*[19] (Table 3, error ±0.1[+]) the BEDT-TTF charges estimated based on the C=C and C–S bond lengths are ~3/4[+] for donors B and C, and ~1/3[+] for donor A. This would suggest an overall charge for the (BEDT-TTF)_5 pentamer ..ABCBA.. of 3.33[+] in **Tb** at 293 K, and 3.28[+] in **Dy** at 30 K, to balance the charge of the single $[Ln(clo)_3]^{3-}$ anion. Donor A has a disordered ethylene group at both ends of the molecule in **Tb** at 293 K, and also in **Dy** at 30 K. Donor A is located next to the cavities in the neighbouring anion layers at both ends of the donor molecule (Fig. 6), whilst donor C is adjacent to the lanthanide metal centres.

Fig. 7 shows the insulating layer in the *bc* plane consisting of $[Ln(clo)_3]^{3-}$ anions with ethanol and water molecules.

Both enantiomers of the $[Ln(clo)_3]^{3-}$ anion (Table 4) are present in a 50 : 50 ratio (Fig. 7). Within a single anion layer there are rows of a single enantiomer in the *b* direction, with each adjacent row in the *c* direction consisting of the opposing enantiomer to give an overall racemic lattice.

The O atom of the ketone on the periphery of the clo ligand is sandwiched by the two clo ligands of the next nearest $[Ln(clo)_3]^{3-}$ anion, in which a distance between the O atom (O9, Fig. S1†) of the ketone and a carbon atom (C26) of the carboxylate of the nearest $[Ln(clo)_3]^{3-}$ anion is less than 3.0 Å, O9···C26 = 2.793(2) Å for **Dy** and 2.841(4) Å for **Tb**, which is 0.43 and 0.38 Å shorter than the van der Waals distance of C and O, respectively. This suggests a mesomeric aromatic structure with a positive charge on the O atom of the pyrene ring and a negative charge on the ketonic O atom at position 4. This strong interaction produces a 1D chain of the $[Ln(clo)_3]^{3-}$ anion, each of which is connected by the ketone-to-plane interaction of the clo giving a 2D structure where the clo has a short contact with another clo with ketone-to-plane distance (distance between O5 and plane) of

**Table 2** Short range interactions (VdW radii) for donor cations in salt **Tb** at 293 K and **Dy** at 30 K

| Contact/Å | **Tb** | **Dy** |
| --- | --- | --- |
| S1···S12 | 3.649(1) | 3.587(1) |
| S1···S17 | 3.540(2) | 3.490(1) |
| S2···S12 | 3.520(2) | 3.481(1) |
| S4···S19 | 3.504(1) | 3.505(1) |
| S4···S20 | 3.421(2) | 3.367(1) |
| S5···S15 | 3.549(2) | 3.471(1) |
| S5···S17 | 3.463(2) | 3.425(1) |
| S5···S18 | 3.491(1) | 3.453(1) |
| S7···S20 | 3.558(1) | 3.486(1) |
| S8···S20 | 3.420(2) | 3.368(1) |
| S9···S13 | 3.571(2) | 3.564(1) |
| S10···S13 | 3.440(1) | 3.564(1) |
| S12···S15 | 3.499(1) | 3.414(1) |
| S12···S16 | 3.562(2) | 3.471(1) |

**Table 3** Approximation of the charge on the BEDT-TTF molecules in salts **Tb** and **Dy** using the average bond lengths. $\delta = (b + c) - (a + d)$, $Q = 6.347 - 7.463\delta$ [18]



| Salt | Donor | $a$ | $b$ | $c$ | $d$ | $\delta$ | $Q$ |
|------|-------|-----|-----|-----|-----|----------|-----|
| **Tb** | A | 1.361 | 1.74575 | 1.75675 | 1.340 | 0.801 | 0.37 |
| | B | 1.377 | 1.72325 | 1.7425 | 1.3575 | 0.731 | 0.89 |
| | C | 1.390 | 1.7195 | 1.769 | 1.357 | 0.742 | 0.81 |
| | | | | | | | ABCBA = 3.33[+] |
| **Dy** | A | 1.366 | 1.75525 | 1.76375 | 1.3545 | 0.799 | 0.39 |
| | B | 1.381 | 1.74175 | 1.76075 | 1.359 | 0.763 | 0.656 |
| | C | 1.383 | 1.7375 | 1.756 | 1.366 | 0.745 | 0.79 |
| | | | | | | | ABCBA = 3.28[+] |

The anion has a charge of 3- to be balanced by the charge of 5BEDT-TTFs (ABCBA).

**Table 4** Bond lengths and angles of Ln(clo)$_3$ anion

| Ln–O bond lengths/Å | | | |
|---|---|---|---|
| Tb1–O1 | 2.351(3) | Dy1–O1 | 2.326(3) |
| Tb1–O2 | 2.587(3) | Dy1–O2 | 2.562(3) |
| Tb1–O3 | 2.336(3) | Dy1–O3 | 2.335(3) |
| Tb1–O7 | 2.365(2) | Dy1–O7 | 2.360(3) |
| Tb1–O8 | 2.554(4) | Dy1–O8 | 2.578(3) |
| Angle between ligands/° | | | |
| O1–Tb1–O3 | 83.00(10) | O1–Dy1–O3 | 83.41(9) |
| O3–Tb1–O7 | 79.79(10) | O3–Dy1–O7 | 82.65(9) |
| O1–Tb1–O7 | 78.52(9) | O1–Dy1–O7 | 79.05(9) |
| Bite angle of ligands/° | | | |
| O1–Tb1–O3 | 123.38(10) | O1–Dy1–O3 | 125.44(9) |
| O7–Tb1–O7 | 125.86(12) | O7–Dy1–O7 | 125.55(12) |

3.065 for **Dy** and 3.132 Å for **Tb**, which is only 0.1–0.2 Å shorter than the van der Waals distance between C and O. The reason why O9 has strong interaction with the carbon atom of –COO⁻ but O5 has no strong contact with the carbon atom of ketone is as follows. As shown in Fig. S1a,† clo with O9 is almost planar, the dihedral angle between the six-membered ring and two –COO⁻ groups of 0.85° for **Dy** and 0.03° for **Tb** were observed, so that conjugation, namely back donation effect, can widely spread over the clo ligand including the ketone group, namely O9. On the other hand, the clo ligand with O5 is bent as shown in Fig. S1b,† the dihedral angle of 20.92° for **Dy** and 15.61° for **Tb** was observed, therefore conjugation, donation and back donation effects, spreads only over –COO⁻ groups and O5 has no back donation effect. It is totally consistent that the carbon atom of the –COO⁻ has a very short contact with O9 having the effect of back donation. The 2D anion arrangement provides a cavity (see red circle in Fig. 7), in which the ethylene of donor A of the BEDT-TTF pentamer is located.

Despite salts **Tb** and **Dy** being isomorphous they exhibit different conducting behaviour. The resistivity curve of salt **Tb** has an anomaly at 250 K as shown in Fig. 8 upper. The Arrhenius plots are shown in Fig. 8 lower. The expansion of
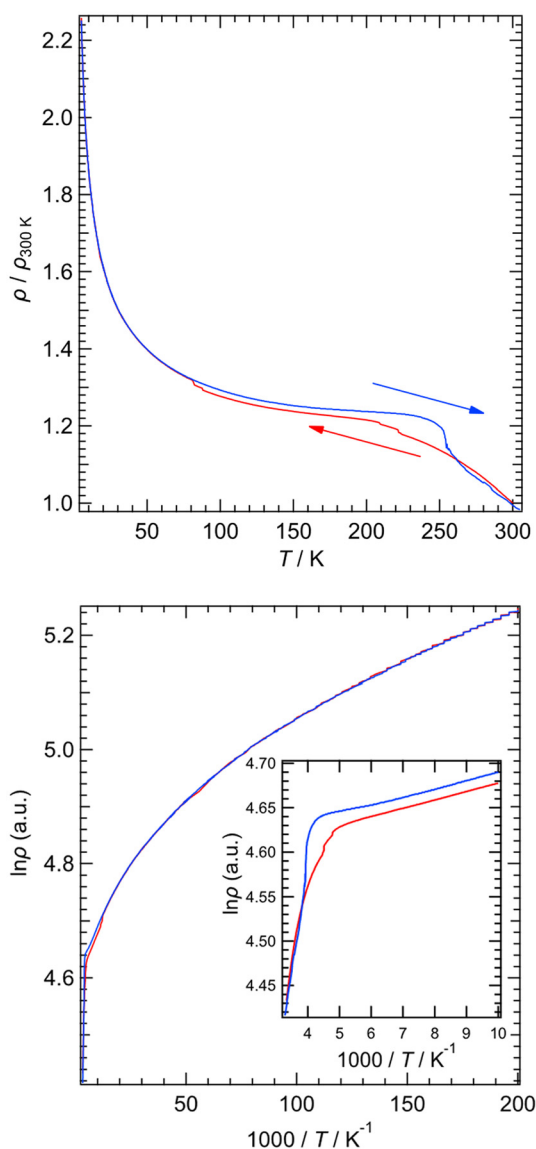


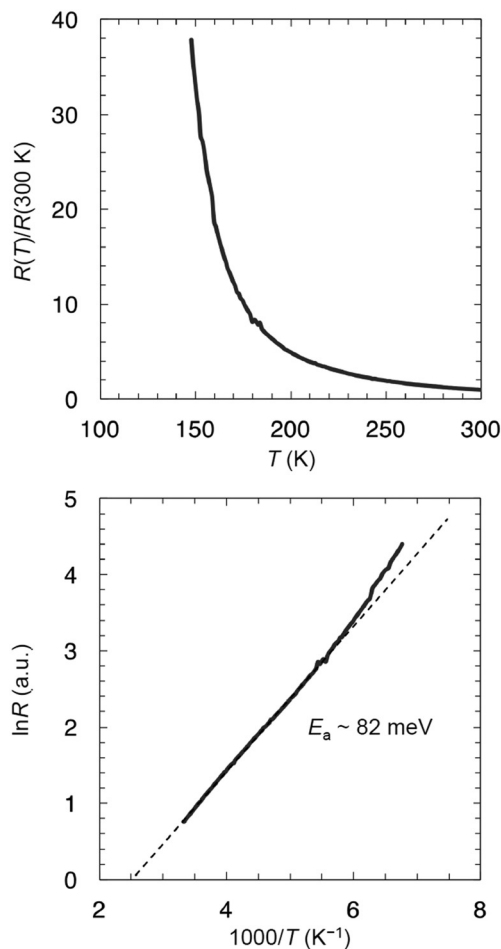**Fig. 8** Electrical resistivity for **Tb**.

**Fig. 9** Electrical resistivity for **Dy**.

the high temperature region is shown in the inset of Fig. 8 lower. The activation energy above 250 K (260 K–RT) is calculated to be 34 meV, which is unusually higher than that below 250 K (100–166 K) of 13 meV (see the inset of Fig. 8 lower). The Arrhenius plots below 250 K (Fig. 8 lower) suggest that the activation energy decreases with decreasing temperature to

0.14 meV from 5–6.6 K, which is approximately 1/100 and 1/250 times smaller than that at just below or just above 250 K. This tendency is not that of a semiconductor, which is normally an insulator at the lowest temperature, but for a metal or semimetal. In the circumstance, we believe that salt **Tb** is a semimetal. Whilst salt **Dy** shows semiconducting behaviour with an activation energy of ~82 meV (Fig. 9) and the salt is an insulator at the lowest temperatures. These conducting properties are consistent with the band structure for both **Tb** (Fig. 10) and **Dy** (Fig. 11) (overlap integrals for **Tb** and **Dy** are provided in Fig. S2†). The band structure for **Tb** (Fig. 10) has 1D, quasi-1D (= between 1D and 2D) and 2D Fermi surfaces. Whilst the band structure for **Dy** has only 1D and 2D Fermi surfaces. The highest two dispersion lines of **Dy**, whose bandwidth is approx. 0.115 eV, is approximately 10% narrower than those of **Tb**, 0.127 eV. Therefore, the highest two dispersion lines of **Tb** and the Fermi level line cross to provide a quasi-1D band, whereas the highest two dispersion lines of **Dy** and the Fermi level line do not cross and therefore there are simpler 1D and 2D Fermi surfaces than those of **Tb**. Moreover, **Tb** has no mid-gap in the band dispersion, suggesting that it is a normal metal and Mott-like charge localisation is not expected. Nesting might occur in this salt, which will be complex because of the three different types of Fermi surfaces, which may cause the anomaly on the resistivity curve at around 250 K. On the other hand, **Dy** has a very small (approximately 13 meV) but significant mid-gap, which separates the upper six dispersion lines and lower four dispersion lines. Therefore, the lower four dispersion lines are fully occupied by electrons and the upper six dispersion lines has six holes (= six electrons), indicating it is effective half filled. In the circumstance, the salt shows simple semiconducting behaviour. In addition, the width of the mid-gap of 13 meV is more than ten times smaller than the gap width calculated from the activation energy ($E_g = 2E_a = 164$ meV), suggesting that electron correlation, which was not concerned in the band calculation, is quite effective for the **Dy** salt. The **Tb** salt is isostructural to the **Dy** salt, therefore the effect of electron correlation is also quite effective for the **Tb** salt.
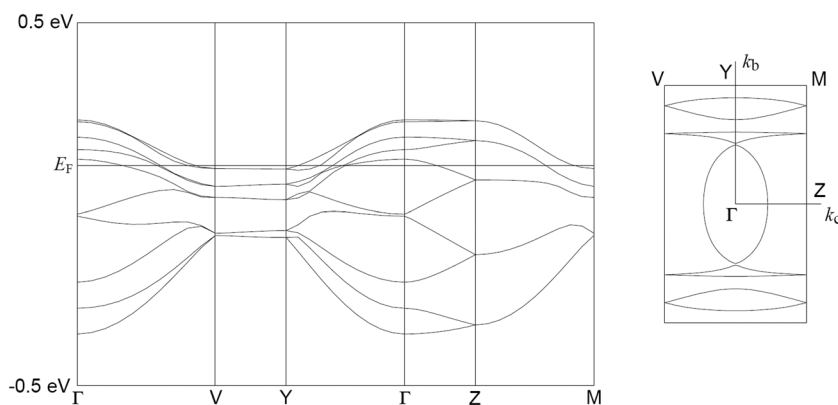


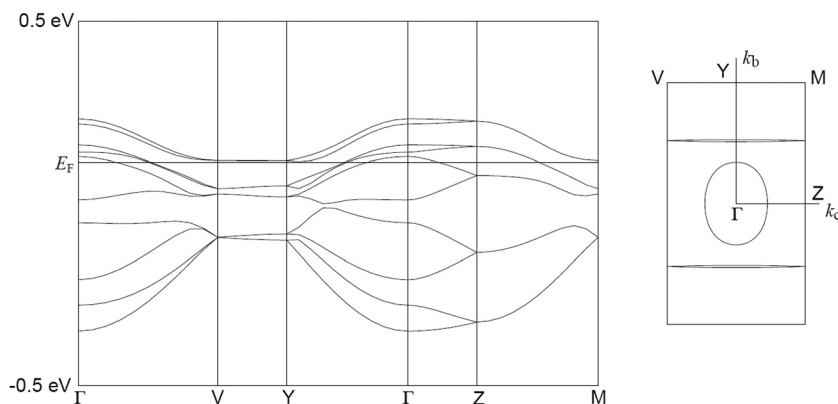**Fig. 10** Band calculation for **Tb** at 293 K.

**Fig. 11** Band calculation for **Dy** at 30 K.

## Conclusions

We report the first BEDT-TTF radical-cation salts with tris-co-ordinated racemic lanthanide(III) anions. These salts are iso-morphous with formula $\alpha$-(BEDT-TTF)$_5$M(clo)$_3$·EtOH·2H$_2$O where M = **Tb** or **Dy**. These are also the first crystallographic determinations of the nine-coordinate tris(chelidonato)terbate and tris(chelidonato)dysprosate anions (chelidonic acid = clo = 4-oxo-4H-pyran-2,6-dicarboxylic acid). Despite BEDT-TTF salts **Tb** and **Dy** being isomorphous they exhibit different conducting behaviour which are consistent with the band structures for both salts. The arrangement of [Ln(clo)$_3$]$^{3-}$ anions within the insulating layer suggests that the six-membered ring has weak aromatic nature. This strong interaction produces a 1D chain of the [Ln(clo)$_3$]$^{3-}$ anion, each of which is connected by the ketone-to-plane interaction of the clo giving a 2D structure where the clo has a short contact with another clo with ketone-to-plane distance (distance between O5 and plane) of 3.065 for **Dy** and 3.132 Å for **Tb**, which is only 0.1–0.2 Å shorter than the van der Waals distance between C and O. Future work will focus on the optimisation of the crystal growth of these salts with **Tb**, **Dy**, as well as other Ln(III) ions, and a study of their magnetic properties.

## Experimental

### Starting materials

Terbium chloride hexahydrate, dysprosium chloride hexa-hydrate, chelidonic acid, sodium hydroxide, chlorobenzene, ethanol and 15-crown-5 were purchased from Sigma-Aldrich and used as received. BEDT-TTF was purchased from TCI and recrystallised from chloroform.

### Synthesis of radical-cation salts

Na$_3$[Tb(clo)$_3$] and Na$_3$[Dy(clo)$_3$] were synthesised by literature methods using chelidonic acid with terbium(III) chloride hexa-hydrate and dysprosium(III) chloride hexahydrate, respect-ively.[20] Radical-cation salts **Tb** and **Dy** were synthesized by dis-solving 120 mg of Na$_3$[Ln(clo)$_3$] with 3 drops of 15-crown-5

ether in 20:5 chlorobenzene:ethanol by stirring overnight. This was filtered into a H-shaped electrochemical cell contain-ing 10 mg BEDT-TTF in the anode compartment. An initial current of 0.1 µA was applied then increased to 0.5 µA after 1 week before black hexagonal crystals were collected after 4 weeks for **Tb** and after 2 weeks for **Dy**.

### Electrical resistivity measurements

Electrical resistance measurements were performed using Physical Properties Measurement System (PPMS). Temperature dependent electrical resistivity measurements were performed using four contacts on single crystals of **Tb** and **Dy** in the range 5 K–300 K for **Tb** and 150 K–300 K for **Dy**. A current of 10 µA was applied in the conduction plane, and in-plane resis-tance was measured. The samples were cooled down at a cooling rate of 1 K min$^{-1}$. For the crystals of **Dy** the resistance data is provided with the unit of Ohms, rather than Ohms.cm, because the length along the long axis was only approximately 0.2–0.3 mm. Consequently, accurately estimating the crystal thickness and the distance between terminals makes it difficult to convert the obtained resistance into resistivity.

### X-ray crystallography†

**Crystal data: Tb.** C$_{73}$H$_{56}$O$_{21}$S$_{40}$Tb$_1$, $M$ = 2710.56, black plate, $a$ = 47.654(2), $b$ = 11.0579(3), $c$ = 21.3658(9) Å, $\beta$ = 120.249(6)°, $U$ = 9725.9(9) Å$^3$, $T$ = 296 K, space group $C2/c$, $Z$ = 4, $\mu$ = 1.653 mm$^{-1}$, reflections collected = 44 369, independent reflec-tions = 8836, $R1$ = 0.0468, w$R2$ = 0.0996 [$F^2 > 2\sigma(F^2)$], $R1$ = 0.0572, w$R2$ = 0.1037 (all data). CCDC 2357688.†

**Crystal data: Dy.** C$_{73}$H$_{56}$O$_{21}$S$_{40}$Dy$_1$, $M$ = 2714.07, black plate, $a$ = 44.9281(9), $b$ = 11.0132(2), $c$ = 20.9971(4) Å, $\beta$ = 113.191(2)°, $U$ = 9549.9(3) Å$^3$, $T$ = 30 K, space group $C2/c$, $Z$ = 4, $\mu$ = 1.723 mm$^{-1}$, reflections collected = 30 702, independent reflec-tions = 10 815, $R1$ = 0.0502, w$R2$ = 0.1195 [$F^2 > 2\sigma(F^2)$], $R1$ = 0.0613, w$R2$ = 0.1268 (all data). CCDC 2357687.†

Data for **Tb** (at 293 K) were collected on a Rigaku Oxford Diffraction Xcalibur System equipped with a Sapphire detector at using the CrysAlisPro software,[21] solved using SHELXT[22] and refined using SHELXL-2017.[23]

Data for **Dy** (at 30 K) were collected on Beamline i19, Diamond Light Source Ltd. 3-Circle fixed chi goniometer equipped with a PILATUS 2 M PIXEL detector, wavelength 0.6998 Å (100 μm focus), solved using SHELXT[24] and refined using SHELXL-2014/7.[25]

Molecular illustrations were prepared with Mercury.[26]

## Author contributions

Synthesis, L. M., E. H., J. L.; X-ray crystallography, J. O. O., T. J. B., H. A., Y. N., S. J. C., P. N. H., J. C.; conductivity measurements S. I., H. A., Y. N., Y. I.; band calculations, H. A.; writing—original draft preparation, L. M., H. A.; project administration, L. M.; funding acquisition, L. M.; supervision, L. M., T. J. B.

## Data availability

Crystallographic data for **Tb** and **Dy** has been deposited at the CCDC 2357688 and 2357687.†

## Conflicts of interest

There are no conflicts to declare.

## Acknowledgements

## References

1 J. M. Williams, J. R. Ferraro, R. J. Thorn, K. D. Carlson, U. Geiger, H. H. Wang, A. M. Kini and M. H. Whangbo, *Organic Superconductors: Synthesis, Structure, Properties and Theory*, Prentice Hall, Englewood Cliffs, NJ, 1992.

2 E. Coronado and P. Day, *Chem. Rev.*, 2004, **104**, 5419–5448.

3 P. Day, M. Kurmoo, T. Mallah, I. R. Marsden, R. H. Friend, F. L. Pratt, W. Hayes, D. Chasseau, J. Gaultier, J. Bravic and L. Ducasse, *J. Am. Chem. Soc.*, 1992, **114**, 10722–10729.

4 M. Kurmoo, A. W. Graham, P. Day, S. J. Coles, M. B. Hursthouse, J. L. Caulfield, J. Singleton, F. L. Pratt, W. Hayes, L. Ducasse and P. Guionneau, *J. Am. Chem. Soc.*, 1995, **117**, 12209.

5 S. Benmansour and C. J. Gómez-García, *Magnetochemistry*, 2021, **7**, 93; L. Martin, *Coord. Chem. Rev.*, 2018, **376**, 277–291.

6 E. Coronado, J. R. Galán-Mascarós, C. J. Gómez-García and V. Laukhin, *Nature*, 2000, **408**, 447–449; A. Alberola, E. Coronado, J. R. Galán-Mascarós, C. Giménez-Saiz and C. J. Gómez-García, *J. Am. Chem. Soc.*, 2003, **125**, 10774–10775.

7 B. Zhang, Y. Zhang and D. Zhu, *Chem. Commun.*, 2012, **48**, 197–199.

8 M. Tamura, F. Matsuzaki, Y. Nishio, K. Kajita, T. Kitazawa, H. Mori and S. Tanaka, *Synth. Met.*, 1999, **102**, 16.

9 O. N. Kazheva, M. Gener, V. V. Gritsenko, N. D. Kushch, E. Canadell and O. A. Dyachenko, *Mendeleev Commun.*, 2001, **11**, 182; O. N. Kazheva, D. N. Kushch, O. A. Dyachenko and E. Canadell, *J. Solid State Chem.*, 2002, **168**, 457–463; S. Ueki, T. Nogami, T. Ishida and M. Tamura, *Mol. Cryst. Liq. Cryst.*, 2006, **455**, 129–134.

10 Y. N. Shvachko, D. V. Starichenko, A. V. Korolyov and N. D. Kushch, *Synth. Met.*, 2008, **158**, 315.

11 M. Tamura, K. Yamanaka, Y. Mori, Y. Nishio, K. Kajita, H. Mori, S. Tanaka, J.-I. Yamaura, T. Imakubo, R. Kato, Y. Misaki and K. Tanaka, *Synth. Met.*, 2001, **120**, 1041–1042.

12 Y. B. Shen, G. Cosquer, B. K. Breedlove and M. Yamashita, *Magnetochemistry*, 2016, **2**, 44; Y. B. Shen, G. Cosquer, H. Zhang, B. K. Breedlove, M. Cui and M. Yamashita, *J. Am. Chem. Soc.*, 2021, **143**, 9543–9550.

13 P. P. Lima, O. L. Malta and S. A. Júnior, *Quim. Nova*, 2005, **28**, 805–808.

14 R. Carballo, A. B. Lago, A. Pino-Cuevas, O. Gómez-Paz, N. Fernández-Hermida and E. M. Vázquez-López, *Chemistry*, 2021, **3**, 256–268.

15 C.-M. Liu, J. Xiong, D.-Q. Zhang, B.-W. Wang and D.-B. Zhu, *RSC Adv.*, 2015, **5**, 104854–104861.

16 L. Martin, P. Day, P. N. Horton, S. Nakatsuji, J. Yamada and H. Akutsu, *J. Mater. Chem.*, 2010, **20**, 2738–2742; L. Martin, H. Akutsu, P. N. Horton, M. B. Hursthouse, R. W. Harrington and W. Clegg, *Eur. J. Inorg. Chem.*, 2015, 1865–1870.

17 T. J. Blundell, M. Brannan, H. Nishimoto, T. Kadoya, J.-I. Yamada, H. Akutsu, Y. Nakazawa and L. Martin, *Chem. Commun.*, 2021, **57**, 5406–5409; T. J. Blundell, K. Sneade, J. R. Lopez, J. D. Wallis, H. Akutsu, Y. Nakazawa, S. J. Coles, C. Wilson and L. Martin, *Dalton Trans.*, 2022, **51**, 4843–4852.

18 A. L. Morritt, J. R. Lopez, T. J. Blundell, E. Canadell, H. Akutsu, Y. Nakazawa, S. Imajo and L. Martin, *Inorg. Chem.*, 2019, **58**, 10656–10664.

19 P. Guionneau, C. J. Kepert, G. Bravic, D. Chasseau, M. R. Truter, M. Kurmoo and P. Day, *Synth. Met.*, 1997, **86**, 1973–1974.

20 C. Reinhard and H. U. Guidel, *Inorg. Chem.*, 2002, **41**(5), 1048; P. P. Lima, O. L. Malta and S. Alves Júnior, *Quim. Nova*, 2005, **28**(5), 805–808.

21 CrysAlisPRO, Oxford Diffraction/Agilent Technologies UK Ltd, Yarnton, England.

22 G. M. Sheldrick, SHELXT Version 2014/5, *Acta Cryst.*, 2014, **70**, C1437.

23 G. M. Sheldrick, SHELXL Version 2017/1, *Acta Crystallogr., Sect. A:Found. Crystallogr.*, 2008, **64**, 112–122.

24 G. M. Sheldrick, SHELXT, *Acta Crystallogr., Sect. A:Found. Adv.*, 2015, **71**, 3–8.

25 G. M. Sheldrick, *SHELXL97*, University of Göttingen, Germany, 1997.

26 C. F. Macrae, P. R. Edgington, P. McCabe, E. Pidcock, G. P. Shields, R. Taylor, M. Towler and J. van de Streek, *J. Appl. Crystallogr.*, 2006, **39**, 453–457.